Intrinsic Viscosity of Oligo- and Polystyrenes

Yoshiyuki Einaga, Hitoshi Koyama, Toshiki Konishi, and Hiromi Yamakawa*

Department of Polymer Chemistry, Kyoto University, Kyoto 606, Japan.
Received November 23, 1988; Revised Manuscript Received February 6, 1989

ABSTRACT: The intrinsic viscosity $[\eta]$ was determined in the range of weight-average molecular weight M_w from about 10 000 to 266 (the dimer) for narrow-distribution atactic α-hydro-ω-butylpolystyrene (a-PS) of fixed stereochemical composition in cyclohexane at 34.5 °C and in benzene at 25.0 °C. The results showed that $[\eta]$ of a-PS followed the familiar relation $[\eta] \propto M_w^{1/2}$ for M_w larger than 4000 for the cyclohexane solutions and for M_w from 1500 to 5400 for the benzene solutions but deviated at lower M_w. The theory of $[\eta]$ based on the helical wormlike (HW) touched-bead model could explain quantitatively the observed molecular weight dependence of $[\eta]$ for M_w larger than 900 (which corresponds to the octamer) and gave the values of the HW model parameters for a-PS in cyclohexane and in benzene. The model parameters thus obtained gave the conclusion that the unperturbed mean-square radius of gyration $\langle S^2 \rangle$ of a-PS was larger in benzene than in cyclohexane by about 5%, when compared at the same M_w. The critical number n_K of Kuhn statistical segments above which the excluded-volume effect becomes appreciable was calculated to be about 6.5 from the critical value 5500 of M_w estimated from the experimental $[\eta]$ data in benzene. The value is almost 1 order of magnitude smaller than Norisuye and Fujita's estimate $n_K \simeq 50$ and close to the prediction by Yamakawa and Shimada. The HW chain model with the parameter values determined rendered visible the conformation of the a-PS chain in dilute solution. It was found that the Kratky–Porod model must be given up to represent the a-PS chain, although it has been often adopted for analyzing solution properties of short flexible polymers.

Introduction

Dimensional and transport properties of flexible polymers in dilute solution have for long been studied mainly concerning the excluded-volume effects.[1] In these studies, a highly coarse-grained model, i.e., a random-flight or Gaussian chain, has been employed to analyze experimental data. The so-called two-parameter treatment based on such a model suffices for our understanding of the global properties of long flexible polymers. However, the details of the chemical structure of real polymer chains are smeared out there and reflected only in the value of the (unperturbed) mean-square radius of gyration $\langle S^2 \rangle$ or the Kuhn (or Gaussian) segment length.

One of the purposes of a study on solution properties of flexible polymers is to determine the average shape or conformation of a given polymer chain in solution. To this end, we can now adopt three polymer chain models, i.e., the rotational-isomeric state (RIS) model,[2] the Kratky–Porod (KP) wormlike chain,[3] and the helical wormlike (HW) chain,[4,5] which are different from each other in the extent of the coarse graining. The RIS model takes into account the details of the chain structure on the atomic level. It is, however, inconvenient to treat equilibrium and transport (or dynamical) properties in a consistent manner, and moreover, such details are often unnecessary to consider. In contrast to this, the detailed chemical structure of the real polymer chain is smeared out in the KP chain as in the random-flight model. Although the KP chain can treat both static and transport properties in a simple manner, it can be applied not to asymmetric polymers but only to polymers of highly axial symmetry. On the other hand, the HW chain covers a wide variety of polymers without any restriction, including the KP chain as a special case. It enables us to describe the equilibrium conformational and transport behavior of a real polymer chain on the bond length or somewhat longer scale and thus coarse grains the detailed chemical structure to a lesser extent than does the latter.

The adaptation of the model to a given polymer depends on the length scale on which the molecular structure is experimentally detected, and the length scale depends on what property is studied. In this respect, it can be said that the HW chain is the best model at the present time to explore the correlation between the chemical structure and solution properties of individual real polymers. A number of theories[4,5] based on the HW model have been developed to formulate various observables such as $\langle S^2 \rangle$, mean-square optical anisotropy $\langle \Gamma^2 \rangle$, intrinsic viscosity $[\eta]$, sedimentation coefficient s, translational diffusion coefficient D, and so forth for various polymer chains without excluded volume. The analysis of the experimental results for them with the corresponding theories allows us to determine the model parameters of the HW chain and to obtain therefrom information concerning the three-dimensional structure of a given real polymer chain, by representing its contour as a space curve. The model parameters are the differential-geometrical curvature κ_0 and torsion τ_0 of the characteristic regular helix which the HW chain contour takes at the minimum zero of its elastic energy, the static stiffness parameter λ^{-1}, and the shift factor M_L defined as the molecular weight per unit contour length. In addition to these, we need another parameter representing the finite thickness of the chain in the treatment of transport properties, where the HW cylinder model of cylinder diameter d or touched-bead model of bead diameter d_b is used.

In a previous paper,[6] we experimentally determined the mean-square optical anisotropy $\langle \Gamma^2 \rangle$ of atactic polystyrene (a-PS) at infinite dilution over a wide range of molecular weight, including the oligomer region, with samples of narrow molecular weight distribution and fixed stereochemical composition (the fraction of racemic dyads f_r = 0.59 ± 0.01). The HW chain theory of $\langle \Gamma^2 \rangle$ has been successfully applied to the experimental data to give the values of the model parameters for the a-PS chain: $\lambda^{-1}\kappa_0 = 3.0 \pm 1$, $\lambda^{-1}\tau_0 = 6.0 \pm 1$, $\lambda^{-1} = 22.7 \pm 2$ Å, and $M_L = 37.1 \pm 1$ Å^{-1}. Theoretical calculations of $\langle \Gamma^2 \rangle$ with the results well reproduced the observed data at molecular weights larger than the pentamer. It was found that the shape of the a-PS chain in dilute solution is significantly different from that of, for example, atactic poly(methyl methacrylate) (a-PMMA).

In the present work, we examine the intrinsic viscosity $[\eta]$ of the same a-PS samples as those in the previous work as a function of molecular weight in Θ and good solvents. We carried out measurements of $[\eta]$ in the low molecular weight region from about 10 000 to 266 (the dimer), expecting that the effect of the chemical structure of the a-PS

0024-9297/89/2222-3419$01.50/0

Table I
Values of M_w, M_w/M_n, and f_r for Atactic Oligo- and Polystyrenes

sample	M_w	M_w/M_n	f_r
OS2	266	1.00	
OS3	370	1.00	0.57
OS4	474	1.00	0.60
OS5	578	1.00	0.58
OS6	680	1.00	0.57
OS8	904	1.01	
A1000-b	1480	1.02	
A2500-a′	1780	1.04	
A2500-a	2270	1.05	
A2500-b	3480	1.07	
A5000-3	5380	1.03	
F1-2	10100	1.03	0.59

chain on $[\eta]$ is observed more clearly than in the higher molecular weight region. The reason we performed the viscosity measurements despite the abundant work accomplished already for a-PS is that the literature data in the oligomer region are still scarce and rather fragmentary and that no special attention has been paid to the tacticity of the samples used. Thus, the main purposes of this paper are as follows: (1) to establish experimentally the molecular weight dependence of $[\eta]$ for a-PS of fixed stereochemical composition (f_r = 0.59) in the oligomer region, (2) to examine the range of molecular weight in which the theory of $[\eta]$ can explain the observed results, and (3) to determine the HW model parameters to obtain valuable information about the shape of the a-PS chain in solution.

Experimental Section

Materials. The a-PS samples used in this work are fractions separated from the standard samples A-500, A-1000, A-2500, A-5000, and F-1 supplied from Tosoh Co. Ltd., by preparative gel permeation chromatography (GPC) or fractional precipitation. Most of the samples are the same as used in the study on $\langle\Gamma^2\rangle$.[6] They have an *n*-butyl group at one of the chain ends and hydrogen at the other, and their stereochemical composition f_r is essentially independent of molecular weight as described before.

The weight-average molecular weight M_w of all the samples studied are summarized in Table I together with the ratios of M_w to the number-average molecular weight M_n and also with the values of f_r. Among these samples, the oligostyrene samples OS*x* from the dimer (x = 2) to the pentamer (x = 5) are completely monodisperse. The samples OS3, OS4, and OS5 were confirmed to be actually the trimer, tetramer, and pentamer, respectively, from their ^{13}C NMR spectra. The other oligomers were identified from the location of their peaks distributed continually on the analytical gel permeation chromatogram. The samples OS6 and OS8 were found to contain a certain amount of two adjacent homologues from the GPC measurements. The values of M_w of the oligomer samples were obtained by calculation from their chemical structure.

On the other hand, M_w of the other samples were directly determined from light scattering measurements for their methyl ethyl ketone (MEK) solutions at 25.0 °C with a modified Fica 50 light scattering photometer. The measurements were accomplished at relatively low polymer concentrations in the range from 0.004 to 0.025 g/cm^3, irrespective of the rather low molecular weights of the samples examined. The obtained data were thus analyzed in the ordinary manner, taking into account the effect of anisotropic scattering. Here, the refractive index increment of each sample in MEK at 25.0 °C was measured with a Shimadzu differential refractometer. The values of the ratio M_w/M_n determined from GPC indicate that the molecular weight distributions of the samples are sufficiently narrow.

The solvents MEK, cyclohexane, and benzene used for light scattering and viscosity measurements were thoroughly purified by the standard procedure prior to use.

Viscometry. Viscosity measurements were carried out for 12 a-PS samples in cyclohexane at 34.5 °C (Θ) and in benzene at 25.0 °C. Since we were concerned with the samples of very low molecular weights and hence very low intrinsic viscosities, we adopted for the measurements a specially designed four-bulb spiral capillary viscometer of the suspended-liquid type. The viscometer was equipped with a spiral capillary tube of about 100 cm long and 0.5-mm i.d. and four bulbs of different capacity aligned vertically. The flow times of pure cyclohexane and benzene at the above temperatures were about 1700 and 1150 s, respectively, when the four bulbs were used as a whole. The actual measurements were made at polymer concentrations corresponding to specific viscosities η_{sp} ranging from 0.01 to 0.1. This range of η_{sp} is about 1 order of magnitude smaller than that in ordinary measurements. However, there still remained flow time differences larger than 10 s between the solution and solvent even at the smallest η_{sp}. The flow time was measured to a precision of 0.1 s, and the test solution was maintained at constant temperature within ±0.003 °C during the measurements.

The polymer mass concentration c of the solution was varied in the range 0.003–0.03 g/cm^3. Density corrections were applied to the solutions in the calculations of c and also of the relative viscosity η_r from the flow times of the solution and solvent with the densities. The solution density was measured as a function of c for each sample and solvent with a picnometer of the Lipkin-Davison type.

The obtained data for η_{sp} and η_r for each sample were processed in the conventional way by the Huggins and Fuoss–Mead plots to evaluate $[\eta]$. Each plot gave a curve bent upward only slightly and allowed us to determine the value of $[\eta]$ with sufficient accuracy.

Table II
Results of Viscometry on Atactic Oligo- and Polystyrenes in Cyclohexane at 34.5 °C and in Benzene at 25.0 °C

	cyclohexane (34.5 °C)		benzene (25.0 °C)	
sample	$[\eta]$, dL/g	k'	$[\eta]$, dl/g	k'
OS2	0.0149	1.3	0.0170	0.79
OS3	0.0192	1.2	0.0218	0.85
OS4	0.0247	0.91	0.0245	0.82
OS5	0.0274	0.89	0.0264	0.82
OS6	0.0293	0.84	0.0280	0.82
OS8	0.0326	0.87	0.0307	0.81
A1000-b	0.0370	0.96	0.0356	0.75
A2500-a′	0.0408	0.94	0.0384	0.77
A2500-a	0.0450	0.89	0.0445	0.73
A2500-b	0.0543	0.93	0.0550	0.71
A5000-3	0.0659	0.81	0.0695	0.58
F1-2	0.0900	0.67	0.102	0.54

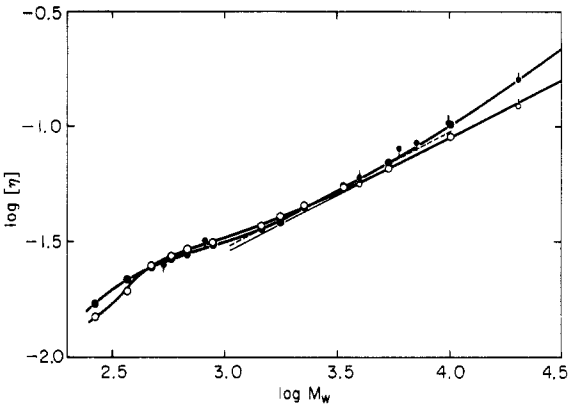

Figure 1. Double-logarithmic plots of $[\eta]$ (in dL/g) against M_w for a-PS in cyclohexane at 34.5 °C (unfilled circles) and in benzene at 25.0 °C (filled circles). No pip, present work; pip down, Altares et al.;[7] pip up, Einaga et al.[8] The thin solid and dashed lines were drawn with a slope of 0.5.

Results

The intrinsic viscosity data for all the a-PS samples determined in the two solvents are summarized in Table II together with the Huggins coefficient k'. They are double-logarithmically plotted against M_w in Figure 1,

which includes the data by Altares et al.[7] for the a-PS samples prepared by the same techniques and hence having the same end groups and also those by Einaga et al.[8] for samples of the same origin as ours. We note that the data of Altares et al. are plotted against M_n instead of M_w, since they measured only the values of M_n of their samples. The literature data are in good agreement with the present ones.

In Figure 1, several new aspects are found for the relationship between $[\eta]$ and M_w. The well-known Mark–Houwink–Sakurada relation $[\eta] = KM_w^a$ is not followed by the two sets of data in different solvent conditions in the range of M_w examined here, although it is well established to hold for higher molecular weights. This finding clearly demonstrates that the relation does not necessarily hold over the whole range of molecular weight even for the typical flexible polymer in the Θ state. For the cyclohexane solutions, the data points fall on a straight line with a slope of 0.5 at M_w larger than about 4000, but deviate upward from the straight line, following a curve slightly bent upward at smaller M_w, and then follow a curve convex upward as the molecular weight is further decreased.

The results for the benzene solutions show a molecular weight dependence of $[\eta]$ qualitatively similar to those for the cyclohexane solutions in the region of M_w lower than about 1500. In this region, the values of $[\eta]$ in the two solvents are close to each other except for the two lowest molecular weight samples, but a detailed comparison reveals that they vary with M_w in a delicately different manner depending on the solvent. It is clearly seen that $[\eta]$ in benzene undergoes the excluded-volume effect in the high molecular weight region of this graph. This effect fades as M_w is decreased and completely vanishes at M_w of about 3000, where $[\eta]$ in benzene is slightly smaller than that in cyclohexane at Θ. It is, however, not easy to determine unequivocally up to what molecular weight the behavior of the unperturbed a-PS chain persists in the $[\eta] - M_w$ relation for the benzene solution. In this regard, we can find from a careful examination of the plot that the data points for the benzene solutions follow a straight line with a slope of 0.5 in the range of M_w from 1500 to 5400. Thus, it may be reasonable to conclude that the a-PS chain in benzene is perturbed by the excluded-volume effect at M_w greater than about 5500. In the linear portion of the plot, $[\eta]$ in benzene is larger than that in cyclohexane by about 6% when compared at fixed M_w. This implies that the properties of the unperturbed a-PS chain slightly depend on the solvent. Here, it is pertinent to point out that the literature data[8-10] of $[\eta]$ and $\langle S^2 \rangle$ of polystyrene are slightly larger (by about 4–5%) in cyclohexane at Θ than in *trans*-decalin at Θ.

It should be emphasized that the present experimental findings on the detailed molecular weight dependence of $[\eta]$ in the oligomer region were made possible for the first time by the careful preparation of the test samples and precise viscometry.

Discussion

Intrinsic Viscosity of the HW Chain. Recently, Yoshizaki et al.[11] have developed a viscosity theory for the HW chain on the basis of the touched-bead model with finite bead volume, thereby supplementing their own previous theory[12] for the HW cylinder. The latter theory has given the numerical solutions for the HW chain of contour length L for large L/d and small λd, so that it cannot be applied to short flexible chains. This is due to the failure of the numerical solution there. On the other hand, the former theory has yielded numerical values of $[\eta]$ for $1 \leq N \leq 1000$ and λd_b ranging from 0.01 to 0.8,

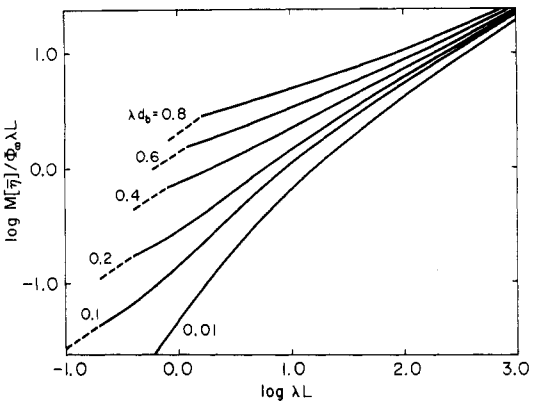

Figure 2. Double-logarithmic plots of the theoretical $M[\bar{\eta}]/\Phi_\infty \lambda L$ against λL for the indicated values of λd_b and for $\lambda^{-1}\kappa_0 = 3.0$ and $\lambda^{-1}\tau_0 = 6.0$.[9] The solid curves represent the values calculated for $N \geq 2$. The dashed lines connect the theoretical values for $N = 1$ and 2.

where N is the number of beads, and an analytical interpolation formula for $[\eta]$ has been presented on the basis of the numerical results. The two results for large and small L (or N) values can be smoothly joined to each other if we assume $d = 0.74d_b$. Thus, we are now able to analyze the experimental data of $[\eta]$ for any molecular weight including the oligomer region and to determine therefrom the values of the HW chain model parameters κ_0, τ_0, λ^{-1}, M_L, and d_b (or d).

The intrinsic viscosity $[\eta]$ of the HW touched-bead model chain is given by

$$[\eta] = [\eta]_{KR} + [\eta]_E \quad (1)$$

Here, $[\eta]_{KR}$ is the Kirkwood–Riseman intrinsic viscosity of the HW chain and $[\eta]_E$ the intrinsic viscosity of the Einstein sphere given by

$$[\eta]_E = 5\pi N_A N d_b^3/12M \quad (2)$$

where N_A is the Avogadro number and M the molecular weight. The contribution of $[\eta]_E$ to $[\eta]$ progressively increases as the chain becomes shorter in the oligomer region. When all lengths are measured in units of λ^{-1}, the reduced intrinsic viscosity $[\bar{\eta}]$ as a function of λL depends on the reduced parameters $\lambda^{-1}\kappa_0$, $\lambda^{-1}\tau_0$, and λd_b. It is related to the experimental $[\eta]$ by

$$\log [\eta] = \log (M[\bar{\eta}]/\Phi_\infty \lambda L) - \log (\lambda^2 M_L) - 2.542 \quad (3)$$

with

$$\log M = \log (\lambda L) + \log (M_L/\lambda) \quad (4)$$

where $\Phi_\infty = 2.87 \times 10^{23}$. Theoretical relations between $M[\bar{\eta}]/\Phi_\infty \lambda L$ and λL are now made ready to use for various values of $\lambda^{-1}\kappa_0$, $\lambda^{-1}\tau^0$, and λd_b. We note that they coincide with those for the ordinary KP wormlike chain in the particular case of $\kappa_0 = 0$.

The quantities $\lambda^2 M_L$ and M_L/λ (and therefore λ^{-1} and M_L) can be estimated from a best fit of double-logarithmic plots of the theoretical $M[\bar{\eta}]/\Phi_\infty \lambda L$ against λL to those of the observed $[\eta]$ against M, in which the parameters $\lambda^{-1}\kappa_0$, $\lambda^{-1}\tau_0$, and λd_b are properly chosen so that the theoretical curve may give the same shape as the experimental one. The choice of the theoretical curve allows us to determine the values of these three-parameter combinations. The theoretical curve significantly changes its shape with them, especially at small λL, as illustrated in Figure 2 for the case of $\lambda^{-1}\kappa_0 = 3.0$ and $\lambda^{-1}\tau_0 = 6.0$. In the figure, the dashed lines connect the values of $[\eta]$ for $N = 1$ and 2, and the solid curves represent the values of $[\eta]$ for $N \geq 2$. The solid curve is convex upward over the whole range of λL at $\lambda d_b = 0.01$, becomes S-shaped with increasing λd_b (for $0.1 \leq$

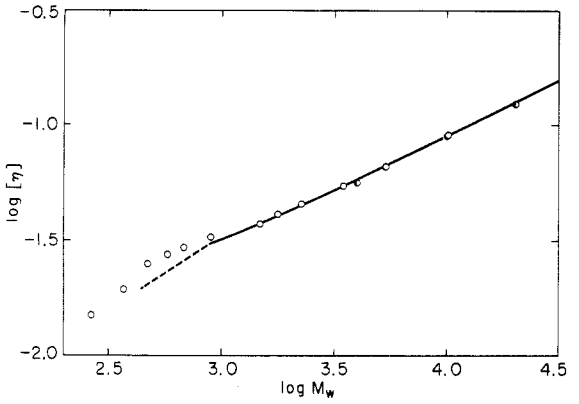

Figure 3. Comparison between the observed and calculated values of $[\eta]$ (in dL/g) for a-PS in cyclohexane at 34.5 °C. Unfilled circles, present work; left-half filled, Einaga et al.[8] The best-fit theoretical values are shown in the solid curve for $N \geq 2$ and the dashed line for $N = 1$ and 2.

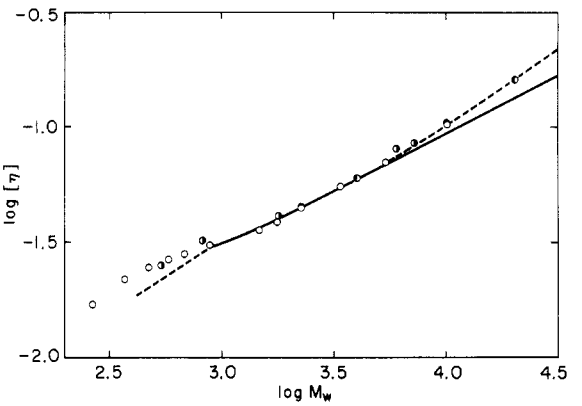

Figure 4. Comparison between the observed and calculated values of $[\eta]$ (in dL/g) for a-PS in benzene at 25.0 °C. Unfilled circles, present work; right-half filled, Altares et al.;[7] left-half filled, Einaga et al.[8] The best-fit theoretical values are shown in the solid curve for $N \geq 2$ and the dashed line for $N = 1$ and 2.

Table III
Values of the HW Model Parameters for Atactic Polystyrene

solvent	T, °C	λ^{-1}, Å	M_L, Å^{-1}	d_b, Å	obsd
cyclohexane	34.5	23.5	42.6	10.1	$[\eta]$
benzene	25.0	24.5	42.1	10.0	$[\eta]$
cyclohexane	34.5	22.7	37.1		$\langle\Gamma^2\rangle$

$\lambda d_b \leq 0.4$), and is convex downward at large λd_b ($\lambda d_b \gtrsim 0.4$). It approaches asymptotically the straight line representing $[\eta] \propto M^{1/2}$ at large λL irrespective of the value of λd_b.

The curve-fitting method was successfully applied to the literature data for a-PMMA and poly(dimethylsiloxane) in various Θ solvents.[11] In particular, all five parameters for a-PMMA were determined from the experimental results only for $[\eta]$ owing to its conspicuous molecular weight dependence at relatively large M_w, although the data points were considerably scattered. In contrast to this, it is difficult to determine all of the model parameters for a-PS from a similar analysis of the present data shown in Figure 1. Thus, in this paper, we assume that $\lambda^{-1}\kappa_0$ and $\lambda^{-1}\tau_0$ are the same as those estimated previously[6] from the analysis of the data for the mean-square optical anisotropy $\langle\Gamma^2\rangle$ in cyclohexane at Θ, i.e., $\lambda^{-1}\kappa_0 = 3.0$ and $\lambda^{-1}\tau_0 = 6.0$, and determine the remaining parameters λ^{-1}, M_L, and d_b. This requires some comments. In this treatment, we implicitly assume that we observe the a-PS chain on the same length scale or to the same degree of coarse graining in viscometry as in anisotropic light scattering photometry. This assumption may be regarded as justified from the fact that both $[\eta]$ and $\langle\Gamma^2\rangle$ are quantities on the same level as the mean-square end-to-end distance or mean-square radius of gyration and that they are studied in the same range of M_w.

Analysis of the Experimental Data. Figure 3 shows the result of the curve fitting for the observed data of $[\eta]$ in cyclohexane at 34.5 °C (Θ). The solid curve represents the best-fit theoretical values for the HW touched-bead chain model for $N \geq 2$. The values of λ^{-1}, M_L, and d_b thus determined are listed in Table III. The theoretical curve well explains the observed behavior in the range of M_w above 900 (corresponding to the octamer), especially the upward deviation of the data points at $900 \leq M_w \leq 4000$ from an extrapolation of the straight line with a slope of 0.5 followed at higher M_w. The upward deviation of $[\eta]$ at Θ from the relation $[\eta] \propto M_w^{1/2}$ may be qualitatively explained also by the Gaussian or spring-bead model[13] if the effect of the finite volume of the bead is taken into account. However, the value of M_w at which the deviation occurs is too large when a reasonable value is assigned to the effective bond length. Thus this theory cannot be applied to the present experimental results in a quantitative sense. It may be said that the present success arises from the fact that the local structure of the a-PS chain is properly represented by the HW chain model.

The value of $[\eta]$ calculated for the HW chain consisting of two beads ($N = 2$) is very close to the data point for the octamer. Thus a single bead in the HW touched-bead chain model approximately corresponds to the four monomer units of the a-PS chain. This result implies that the HW model describes the real a-PS chain to such an extent of high resolution.

In Figure 4, the theoretical calculations are compared with the observed results in benzene at 25.0 °C. We put the prerequisite in the comparison that the a-PS chain in benzene behaves as an unperturbed chain up to M_w of 5500 as stated above. The obtained values of λ^{-1}, M_L, and d_b are also summarized in Table III. Here, the values of $\lambda^{-1}\kappa_0$ and $\lambda^{-1}\tau_0$ were again assumed to be 3.0 and 6.0, respectively, although these values referred to a-PS in cyclohexane at Θ. It is thus implicitly assumed that the characteristic regular helix of the a-PS chain does not depend on the solvent.

It is seen that the theoretical curve represents the data points quite well in the range of M_w from 900 to 5500 and that the HW chain with $N = 2$ corresponds to the octamer of a-PS as in the case of a-PS in cyclohexane. At M_w larger than 5500, the data points deviate upward from the theoretical values because of the excluded-volume effect, while the theoretical calculations naturally give a line with a slope of 0.5 there.

The experimental results for the oligomers from the dimer to hexamer in cyclohexane and benzene cannot be explained by the theory with the model parameters determined in this study. In fact, the theoretical value of $[\eta]_E$ for a single bead (represented by the extreme left of the dashed line) is considerably lower than the observed one for the tetramer or trimer in cyclohexane (Figure 3) or in benzene (Figure 4). The discrepancy suggests that these oligomers take a nonspherical or elongated shape in solution on the statistical average. At any rate, the molecular size of the oligomers becomes comparable to that of the solvent as the molecular weight is decreased, and it is evident that the theoretical treatment of the solution viscosity within the framework of classical hydrodynamics breaks down there. The limit of applicability of the theory, i.e., the size of the smallest solute molecule to which the

theory can be applied, cannot be predicted. However, we may conclude from the results of the curve fitting in Figures 3 and 4 that for the a-PS chain the hydrodynamic theory is valid down to at least the octamer.

In Table III are also given the values of λ^{-1} and M_L obtained previously[6] from $\langle\Gamma^2\rangle$, for comparison. The present values of λ^{-1} and M_L for both the cyclohexane and benzene solutions are in reasonable agreement with the previous estimates, although the former values are slightly larger than the latter. The agreement supports our presumption that $[\eta]$ and $\langle\Gamma^2\rangle$ provide information on the detailed structure of the a-PS chain to the same degree of resolution. The ratio of $\langle S^2\rangle$ to M_w for the unperturbed chain with infinite length was calculated from the values of λ^{-1} and M_L from $[\eta]$ combined with $\lambda^{-1}\kappa_0 = 3.0$ and $\lambda^{-1}\tau_0 = 6.0$ from $\langle\Gamma^2\rangle$. It was found that the ratio was larger for a-PS in benzene than in cyclohexane by a factor of about 1.05. This difference well corresponds to the difference between $[\eta]$ in the two solvents mentioned above. Here, Φ_∞ is implicitly assumed to be independent of the solvent. The result may then require a slight modification of the analysis of the excluded-volume effects, especially the expansion factors α_s and α_η, made so far for the a-PS chain.

Now the Kuhn statistical segment length A_K is defined by

$$A_K = \lim_{L\to\infty} \langle R^2\rangle/L \tag{5}$$

where $\langle R^2\rangle$ is the (unperturbed) mean-square end-to-end distance. The present results for λ^{-1} and M_L yield A_K = 19.2 and 20.0 Å for a-PS in cyclohexane and in benzene, respectively. These values are smaller than those of λ^{-1} by about 18%. We note that A_K is generally smaller than λ^{-1} for the HW chain and equal to λ^{-1} only for the KP chain (the HW chain with $\kappa_0 = 0$).[4,5] The rather small difference between A_K and λ^{-1} of a-PS suggests that the a-PS chain does not have a significant helical nature.

In this connection, we make some comments on the recent analysis of Huber et al.[14,15] on the basis of the KP chain of their experimental data for the translational diffusion coefficient D and $\langle S^2\rangle^{1/2}$ for several PS samples of low molecular weights ranging from 1100 to 10700 in d-cyclohexane at Θ and in d-toluene at 20 °C. They obtained therefrom the values of M_L, A_K, and d as 43.0 Å^{-1}, 20 Å, and 8.3 Å, respectively, for PS in cyclohexane, and 45.0 Å^{-1}, 29 Å, and 6.2 Å, respectively, for PS in toluene. From the results, they claimed that the contour length of the KP chain assumed for PS in cyclohexane lies around the end-to-end distance of the PS chain in the all-trans conformation and that the change of solvent from cyclohexane to toluene modifies "the chain stiffness" of PS represented by A_K. The difference between the values of A_K for the toluene and cyclohexane solutions is, however, unpalatably large and gives more than 40% difference between the ratios $\langle S^2\rangle/M$ for the two solvent systems. Such a great dependence of the unperturbed dimension on solvent cannot be accepted from the observed data for $\langle S^2\rangle$ for PS of higher M_w in toluene and the analysis for the excluded-volume effects.[9]

Another comment is concerned with the onset of the excluded-volume effects. With the values of A_K and M_L in benzene in Table III, the critical number n_K of Kuhn statistical segments above which the excluded-volume effects become appreciable is calculated to be about 6.5 from the critical value 5500 of M_w estimated above. This number is almost 1 order of magnitude smaller than Norisuye and Fujita's estimate[16] $n_K \simeq 50$ and close to the Yamakawa–Stockmayer theory prediction for the KP chain or the Monte Carlo simulation results for the RIS chain by Yamakawa and Shimada.[17,18]

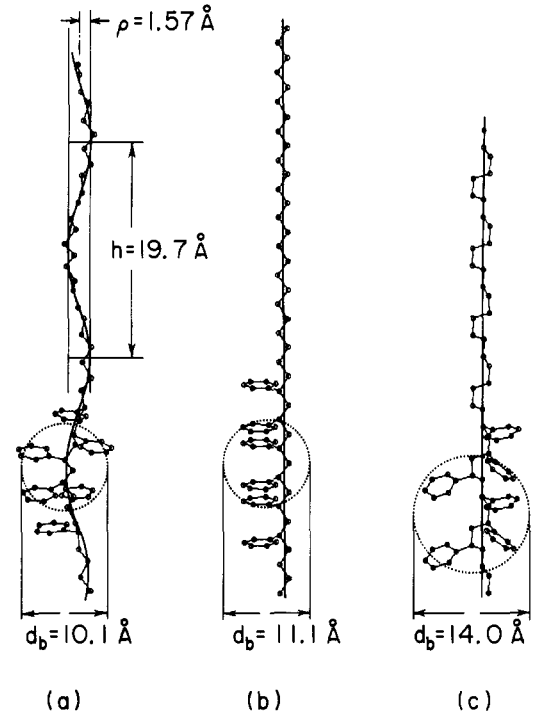

Figure 5. Schematic drawing of the regular structure of the a-PS chain: (a) the HW chain with the model parameters determined in this work; (b) (the KP chain with) the all-trans conformation; (c) the KP chain with the 3_1 helix. In all cases, the portions of the chains displayed include the same number of C–C bonds. The heavy solid line and dotted circle represent the chain contour (characteristic helix) and the hydrodynamic bead, respectively, for each model chain.

Characteristic Helix of a-PS. The radius ρ and pitch h of the regular helix of curvature κ_0 and torsion τ_0 are given by

$$\rho = \kappa_0/(\kappa_0^2 + \tau_0^2) \tag{6}$$

$$h = 2\pi\tau_0/(\kappa_0^2 + \tau_0^2) \tag{7}$$

Those of the characteristic helix of the a-PS chain (in cyclohexane) are then calculated to be 1.57 and 19.7 Å, respectively. Its characteristic helix (heavy solid curve) and conformation (at the minimum of energy) are schematically depicted in Figure 5a, where the large dotted circle represents a (hydrodynamic) bead. The illustration may help understand or picture the conformation of the a-PS chain in dilute solution. (Note that the actual conformation is of course different from the characteristic helix because of thermal fluctuations, their degree being represented by λ.) The remarkable feature of the helix is that the pitch h is quite large compared to the radius ρ. The conformation of a-PS is therefore in sharp contrast to that of a-PMMA, the characteristic helix of which has a very small h and a large ρ.[6,11]

The values of M_L and d_b determined above for the a-PS chain in cyclohexane and in benzene are close to the respective values 40.8 Å^{-1} and 11.0 Å calculated for the chain fully extended to the all-trans conformation, as depicted in Figure 5b. Thus we may conclude that the *local* conformation of the a-PS chain is nearly so in solution. Indeed, the HW chain contour has been taken to coincide with the center line of such a zigzag structure in Figure 5a.

If we adopt the KP chain to analyze our experimental data for $[\eta]$ in cyclohexane, we obtain 20.9 Å, 47.8 Å^{-1}, and 11.1 Å for λ^{-1}, M_L, and d_b, respectively. The value of M_L is approximately equal to the value 48.0 Å^{-1} for the 3_1 helix

of PS as depicted in Figure 5c, when the helix axis is regarded as the KP chain contour. This structure gives the value 14.0 Å for d_b, which is too large compared to the above estimate 11.1 Å for d_b from the experimental $[\eta]$ data. It is therefore hard to accept the structure shown in Figure 5c for the characteristic helix (straight line) of the a-PS chain. Furthermore, it should be emphasized that the KP chain cannot explain the anisotropic light scattering phenomena at all, since in this model, any property that depends on the local structure must be cylindrically symmetric around the chain contour. The above two reasons may suffice to reject the KP chain model in representing the a-PS chain in solution.

In this paper, we have determined the HW model parameters for the a-PS chain and therefrom visualized its local and global conformations in solution. The extension of the study to $\langle S^2 \rangle$ for the same a-PS samples is in progress to confirm the present conclusion.

Registry No. PS, 9003-53-6.

References and Notes

(1) Yamakawa, H. *Modern Theory of Polymer Solutions*; Harper & Row: New York, 1971.
(2) Flory, P. J. *Statistical Mechanics of Chain Molecules*; Interscience: New York, 1969.
(3) Kratky, O.; Porod, G. *Recl. Trav. Chim. Pays-Bas* **1949**, *68*, 1106.
(4) Yamakawa, H. *Ann. Rev. Phys. Chem.* **1984**, *35*, 23.
(5) Yamakawa, H. In *Molecular Conformation and Dynamics of Macromolecules in Condensed Systems*; Nagasawa, M., Ed.; Elsevier: Amsterdam, 1988, p 21.
(6) Konishi, T.; Yoshizaki, T.; Shimada, J.; Yamakawa, H. *Macromolecules* **1989**, *22*, 1921.
(7) Altares, T., Jr.; Wyman, D. P.; Allen, V. R. *J. Polym. Sci., Part A* **1964**, *2*, 4533.
(8) Einaga, Y.; Miyaki, Y.; Fujita, H. *J. Polym. Sci., Polym. Phys. Ed.* **1979**, *17*, 2103.
(9) Berry, G. C. *J. Chem. Phys.* **1966**, *44*, 4550; **1967**, *46*, 1338.
(10) Miyaki, Y.; Einaga, Y.; Fujita, H. *Macromolecules* **1978**, *11*, 1180.
(11) Yoshizaki, T.; Nitta, I.; Yamakawa, H. *Macromolecules* **1988**, *21*, 165.
(12) Yamakawa, H.; Yoshizaki, T. *Macromolecules* **1980**, *13*, 633.
(13) Yamakawa, H. *J. Chem. Phys.* **1970**, *53*, 436.
(14) Huber, K.; Burchard, W.; Akcasu, A. Z. *Macromolecules* **1985**, *18*, 2743.
(15) Huber, K.; Burchard, W.; Bantle, S. *Polymer* **1987**, *28*, 863.
(16) Norisuye, T.; Fujita, H. *Polym. J. (Tokyo)* **1982**, *14*, 143.
(17) Yamakawa, H.; Stockmayer, W. H. *J. Chem. Phys.* **1972**, *57*, 2843.
(18) Yamakawa, H.; Shimada, J. *J. Chem. Phys.* **1985**, *83*, 2607.

Polycondensation Reaction of $RA_a + RB_b$ Type Involving Intramolecular Cyclization

Tang Au-chin, Li Le-sheng, Sun Chia-chung, and Tang Xin-yi*

Institute of Theoretical Chemistry and Department of Chemistry, Jilin University, Changchun, China.

Received April 22, 1988; Revised Manuscript Received January 9, 1989

ABSTRACT: An attempt is made to approach the polycondensation reaction of $RA_a + RB_b$ type, involving intramolecular cyclization, by use of an alternative procedure. The sol fraction for a postgel is investigated to deduce an equilibrium number fraction distribution of the $RA_a + RB_b$ type reaction, with the Stockmayer distribution as a criterion. Furthermore, the zero, the first, and the second polymer moments are evaluated explicitly to reach a gelation condition.

Introduction

As is well-known, the curing theory for polycondensation reactions of $RA_a + RB_b$ and $RA_{a1} \ldots A_{as} + RB_{b1} \ldots B_{bt}$ type has been initiated by Stockmayer.[1,2] Harris, Kilb, Gordon and co-workers, and Ahmad and Stepto[3-7] have studied the polymer system in which intrmolecular cyclization is involved. Miller and Macosko[8,9] have proposed a recursion method in dealing with the problem of postgel properties of network polymers. In this paper, an alternative way to approach the polycondensation reaction of $RA_a + RB_b$ type is proposed, by taking into consideration intramolecular cyclization. The sol fraction for a postgel[8-13] is investigated in detail to deduce an equilibrium number fraction distribution of $(m + l)$-mers. The reliability of this distribution is further examined by the Stockmayer distribution.[2]

It is known that in the theory of branching processes, the probability generating function from differentiation technique proposed by Gordon[14,15] can be used for evaluation of polymer moments. Alternatively, on the basis of the distribution proposed in this paper, a direct differentiation technique is taken to obtain the recursion formula that is suitable for both the pregel and the postgel in evaluating the polymer moments explicitly. As a direct result, the gelation condition is obtained and examined with the Stockmayer gelation condition as a criterion.

Sol Fraction and Equilibrium Number Fraction Distribution

Let us consider a polycondensation system which contains two species of monomers A and B with a and b functionalities, respectively. Let S_a and S_b be the sol fractions with respect to A and B species. Let us use p_{ta}, p'_{ta}, p''_{ta} and p_{tb}, p'_{tb}, p''_{tb}, to which the A and B species correspond, to denote the total, sol, and gel equilibrium fractional conversions. Furthermore, each of the conversions p_{ta}, p'_{ta}, p''_{ta} and p_{tb}, p'_{tb}, p''_{tb} can be separated into two parts such that

$$p_{ta} = f_a + p_a \qquad p'_{ta} = f'_a + p'_a \qquad p''_{ta} = f''_a + p''_a \tag{1}$$

$$p_{tb} = f_b + p_b \qquad p'_{tb} = f'_b + p'_b \qquad p''_{tb} = f''_b + p''_b \tag{2}$$

where p_a (p_b) is the fraction of A (B) functionalities that have reacted intermolecularly and f_a (f_b) the fraction of A (B) functionalities that have reacted intramolecularly. It should be noted that as p'_a (p'_b), p''_a (p''_b), f'_a (f'_b), and f''_a (f''_b) are extents of reaction normalized to total number of groups in sol or gel, thus p'_a (p'_b) is defined as the fraction of A (B) functionalities in the sol that have reacted intermolecularly, p''_a (p''_b) as the fraction of A (B) functionalities in the gel that have reacted intermolecularly,

0024-9297/89/2222-3424$01.50/0